

ВИМІРЮВАННЯ ФІЗИКО-ХІМІЧНИХ ПАРАМЕТРІВ РЕЧОВИН

УДК 532.61

APPLICATION OF AXISYMMETRIC PROFILE ANALYSIS FOR MEASURING SURFACE TENSION AT HARMONIC SURFACE OSCILLATIONS

S.A. Zholob^{1)*}, A.V. Makievski²⁾, R.Miller³⁾ and V.B. Fainerman¹⁾

1)–Physicochemical Centre, Donetsk Medical University, 16 Ilych Avenue, Donetsk 83003, Ukraine, e-mail: s_zholob@ukr.net, fainerman@telenet.dn.ua

2)– SINTERFACE Technologies, Volmerstr. 5-7, 12489 Berlin, Germany, e-mail: a.makievski@sinterface.com

3)– MPI for Colloids and Interfaces, 14424 Potsdam/Golm, Germany, e-mail: reinhard.miller@mpikg.mpg.de

Тензіометрія аналізу профілю як розвиток стандартного аналізу осесиметричної форми краплі використана для вимірювання поверхневого натягу рідин методом форм крапель і бульбашок різних конфігурацій. Алгоритм швидкого пошуку застосований для розрахунку ортогональної відстані між точками експериментального профілю і теоретичним профілем. Встановлена прийнятна стабільність результатів в діапазоні до 60% зміни об'єму краплі або бульбашки. За результатами вимірювань оцінені параметри вязкоеластичності.

Ключові слова: рівняння форми краплі, нелінійна оптимізація, пошук мінімальної відстані, тензіометрія аналізу профілю, осциляція поверхневого натягу.

Тензиометрия анализа профиля как развитие стандартного анализа осесимметричной формы капли использована для измерения поверхностного натяжения жидкостей методом форм капель и пузырьков различных конфигураций. Алгоритм быстрого поиска применен для расчета ортогонального расстояния между точками экспериментального профиля и теоретическим профилем. Установлена приемлемая стабильность результатов в диапазоне до 60% изменения объема капли или пузырька. По результатам измерений оценены параметры вязкоэластичности.

Ключевые слова: уравнение формы капли, нелинейная оптимизация, поиск минимального расстояния, тензиометрия анализа профиля, осцилляция поверхностного натяжения.

The profile analysis tensiometry as a development of the standard analysis of axisymmetric drop shape was used for measuring the surface tension of drops and bubbles of different configurations. A “Quick Search” algorithm was applied to calculate the orthogonal distance between the experimental profile points and the theoretical profile. An acceptable stability of the results was established in a range for up to 60% of drop/bubble volume changes. The parameters of the surface visco-elasticity were estimated on the basis of these surface tension measurements.

Key words: Drop shape equation, nonlinear optimization, search for minimum distance, profile analysis tensiometry, surface tension oscillation.

Surface tensions are extensively studied to gain properties of liquid adsorption layers. The drop profile analysis tensiometry (PAT) is superior over other methods for the following reasons:

a) PAT is a contactless method and therefore has a higher accuracy as compared to contact methods, for example ring or plate tensiometry;

b) PAT covers a very large range of surface formation times –from several seconds up to several hours and more, thus allows reaching the

equilibrium state of adsorption layers;

c) PAT requires very small amounts of sample liquids and provides easy temperature control.

The shape of meniscus at a liquid-fluid interface is described by the equation derived [1] from the Laplace equation of capillarity

$$\gamma \left(\frac{d\phi}{dS} + \frac{\sin \phi}{X} \right) = \frac{2\gamma}{b} + \Delta\rho gZ, \quad (1)$$

where γ is the interfacial tension, b is the radius of curvature at the drop apex, $\Delta\rho$ is the density difference between the drop and the surrounding medium, g is the gravitational acceleration constant, X and Z are horizontal and vertical axes respectively, S is a profile length, ϕ is the angle of the profile tangent in respect to the horizontal axis, as shown in Fig.1.

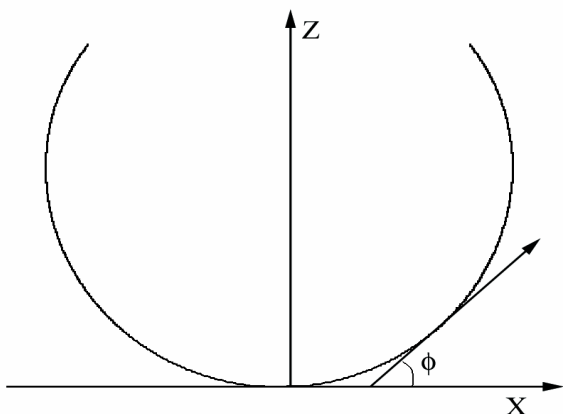


Figure 1 – Schematic view of pendant drop with coordinate axes and radii of curvature

Eq. (1) is a differential equation and for its solution it requires initial conditions which are

$$X(0)=0, Z(0)=0, \phi(0)=0. \quad (2)$$

Dividing both sides of Eq. (1) by γ/b we obtain the following equation as starting point for a calculation algorithm:

$$\frac{d\phi}{ds} = 2 + \beta z - \frac{\sin \phi}{x}, \quad (3)$$

where

$$s = \frac{S}{b}, \quad x = \frac{X}{b}, \quad z = \frac{Z}{b} \quad (4)$$

are dimensionless arc length, horizontal and vertical coordinates respectively, and

$$\beta = \frac{\Delta\rho g b^2}{\gamma} \quad (5)$$

is the dimensionless Bond number. It specifies the shape of the drop, while b serves as a scaling factor. β is regarded to be positive for flattened shapes and negative for elongated ones [1]. So if β and b are known the value of γ is determined as

$$\gamma = \left| \frac{\Delta\rho g b^2}{\beta} \right|. \quad (6)$$

Additionally, any curve is governed by the equations

$$\frac{dx}{ds} = \cos \phi, \quad (7)$$

$$\frac{dz}{ds} = \sin \phi. \quad (8)$$

Eq. (3) has no exact analytical solution. Its first numerical integration was performed manually by Bashforth and Adams [2] who calculated tables of profiles for different values of β . They solved only the direct problem of calculating profiles for given values of β , b , $\Delta\rho$, g , which is nowadays executed on a computer in a few milliseconds or even faster. But the inverse problem of finding the values of β and b which best fit a given profile ($\Delta\rho$ and g are assumed to be known) is much more complicated, though interpolations with the tables of Bashforth and Adams can be used here as well.

All modern techniques of measuring interfacial tension by the drop/bubble shape are based on the solution of the inverse problem. The first and most famous of those techniques is probably the Axisymmetric Drop Shape Analysis (ADSA) developed in the group of A.W. Neumann almost 30 years ago [3]. The schematic view of their set-up is presented in Fig. 2.

Since its first implementation the main parts of ADSA or other devices for measuring interfacial tension are not changed, in principle. Only the digitizing board, initially placed inside a computer, may be excluded now, because video cameras became digital and can transfer already digitized signals to the computer. Also the light source and micro-syringe can be controlled automatically now. Every part of this scheme may be a source of error in measuring interfacial tension [4]. However, in this article we deal only with the software problems denoted by the “Personal computer” block, namely the profile optimization algorithm.

Usually algorithms for measuring the interfacial tension by drop or bubble profile analysis have a general structure as shown in Fig. 4. Some steps may differ or be absent depending on specific algorithm. Our contribution here consists in improving steps 4 and 8.

The coordinates of experimental profile points with an accuracy of about 0,1 pixel were determined as described in [5] by analyzing the grey level gradient across the drop boundary in an image with a Gaussian function

$$G(x) = G_m \exp \left[- \left(\frac{x - x_0}{\sigma} \right)^2 \right], \quad (9)$$

where G_m is considered as a parameter of the image sharpness and x_0 is accepted as the best edge position, while σ describes the gradient change rate. This relates to the block 4 of the algorithm presented in Fig. 4.

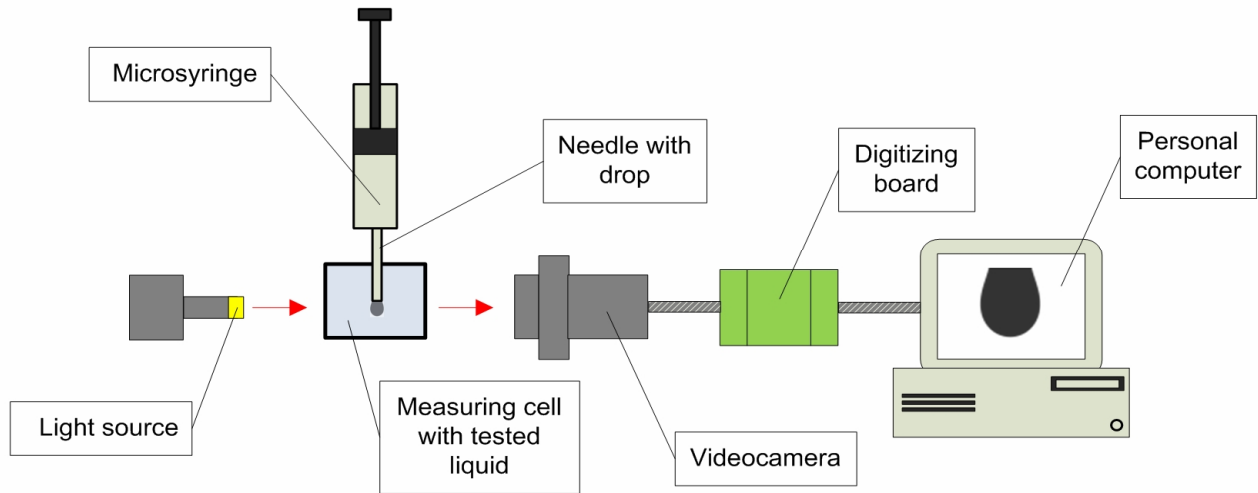


Figure 2 – The schematic view of an ADSA set-up

The algorithm of computing the deviation of experimental profile coordinates to the theoretical profile is as follows (Fig. 3). Input of drop profile coordinates as a list of points determined via a Gaussian approximation (X_i, Z_i) ($i=1..N$) are compared with the theoretical profile comprising of dimensionless points (u_k, v_k) together with ϕ_k ($k=1..M$). Usually $M \gg N$ therefore the theoretical profile totally covers the input profile points. For each point of the input profile an intersection of the normal drawn from the input point to the theoretical profile is found. An intersection interval is found by looking up of the zero crossing of the scalar product

$$p_k = (X_i - X_a - bu_k) \cos(q_k) + (Z_i - Z_a - bv_k) \sin(q_k), \quad (10)$$

where X_a, Z_a are the coordinates of the apex point.

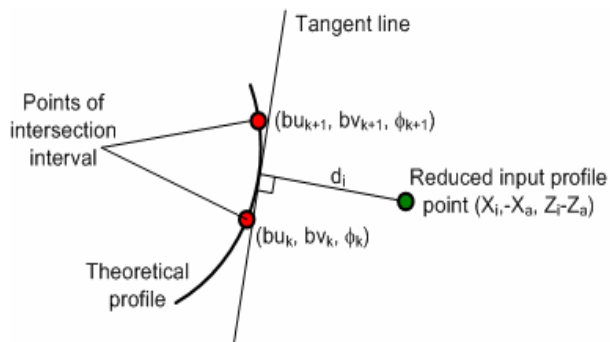


Figure 3 – Layout of look-up for intersection of normal from input point with theoretical profile

To raise the speed of look up the Quick Search algorithm [4] between critical points (equator (for all profiles) and neck point (for elongated profiles, i.e. pendant drops and buoyant bubbles)) is used.

When an interval of nearest theoretical points enclosing zero crossing of the scalar product is found, then the rough intersection point is adjusted by a parabolic approximation. Then a distance between input and intersection point d_i is used for the target function, which is the average sum of squared distances

$$F = \frac{1}{N} \sum_{i=1}^N d_i^2. \quad (11)$$

The distance d_i is regarded to be positive if the input point lies inside the theoretical profile and negative otherwise (as in Fig. 3).

To further boost the calculation a table of pre-calculated profiles as a list of dynamic arrays (each array item contains u, v, ϕ) is used. In this table an average M of about 3000 is used. The value of β is changed in steps of $1/1024$. The number of arrays for pendant drops is 565, and the values are stored without approximation. The number of arrays for sessile drops is 1550, while the values are stored using a Chebyshev approximation [6]. The total file size is 35 MB. After optimization the surface tension value is found via Eq.(6). The Levenberg-Marquardt algorithm of nonlinear optimization given in [7, 8] is then used to find the best-fit parameters. Its detailed implementation can be found elsewhere [9].

It is well known that the accuracy of surface tension measurement depends highly on the drop/bubble volume [10]. In order to determine the range of independence of the measured surface tension on drop volume several special experiments were performed using the drop/bubble profile analysis tensiometer PAT (SINTERFACE Technologies, Germany) [11].

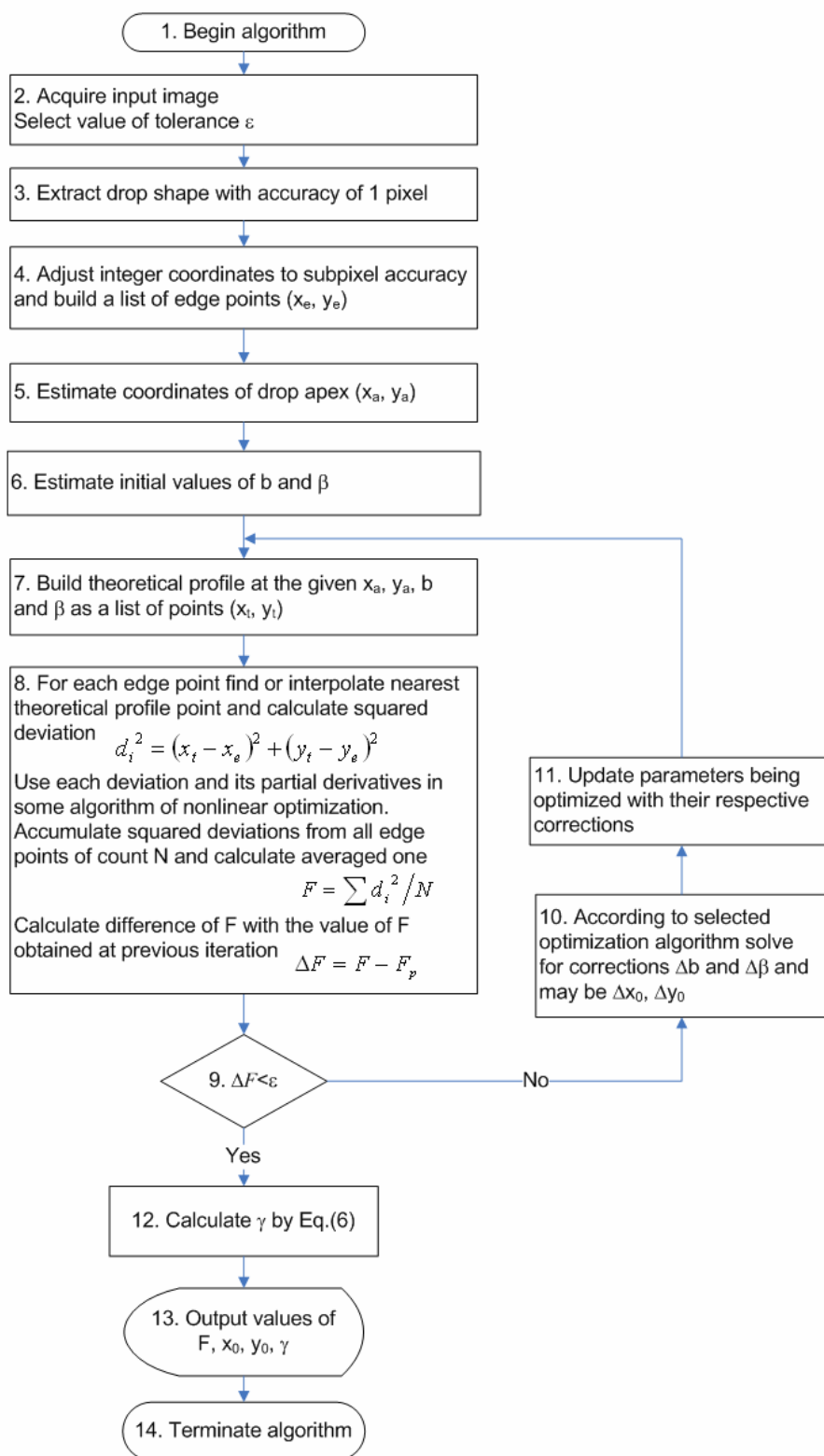


Figure 4 – General structure of the ADSA algorithm

Milli-Q water was used in the first three experiments (2 for bubble and 1 for drop) and a 2 mmol/l solution of Triton-X100 in the fourth one. The dependences of surface tension of pure water and bubble volume are shown in Fig. 5 – for

buoyant bubble as a function of increasing volume and in Fig. 6 for emerging bubble as a function of decreasing volume. The least volume referred to a bubble of almost spherical shape.

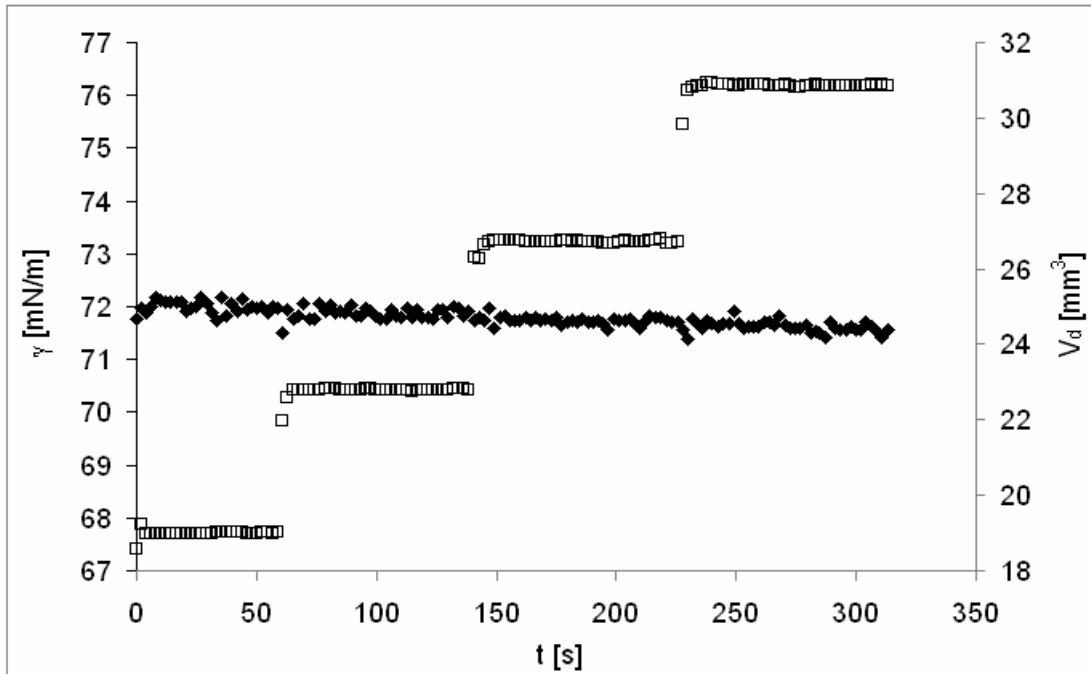


Figure 5 – Dependence of surface tension γ and buoyant bubble volume V_d in pure water as a function of time t , for increasing volume; symbols are: (\blacklozenge) surface tension, (\square) bubble volume

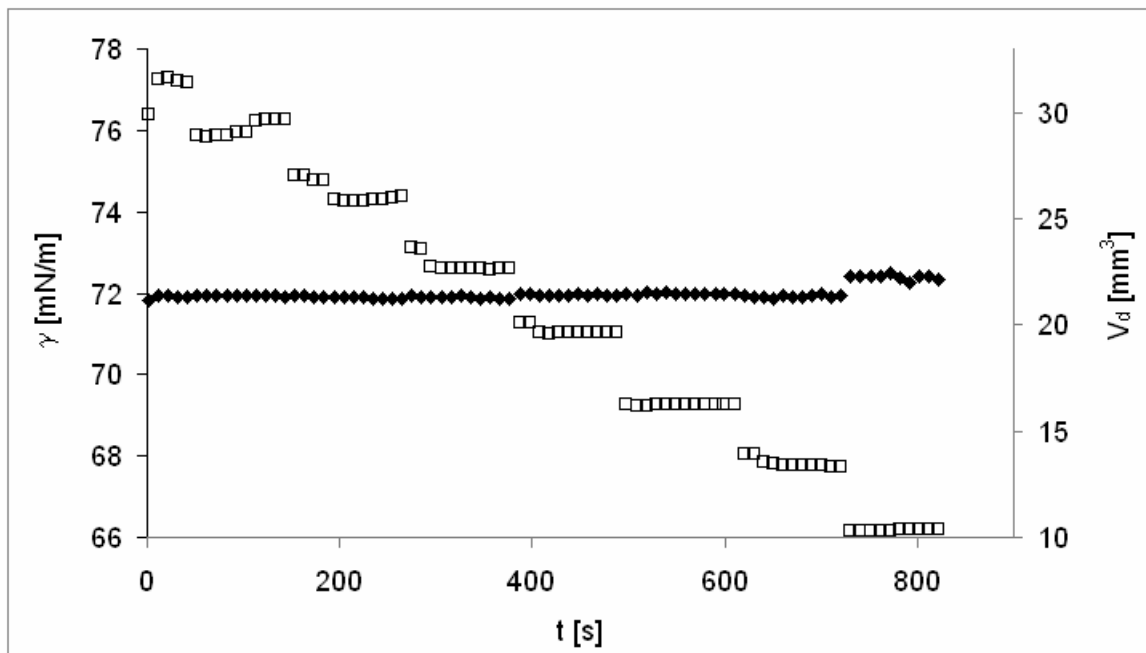


Figure 6 – Dependence of surface tension γ and emerging bubble volume V_d in pure water as a function of time t for decreasing volume; symbols are: (\blacklozenge) surface tension, (\square) bubble volume

As evidenced in Fig. 5 and Fig. 6 there is very little dependence of surface tension on bubble volume. The experiment shown in Fig.7 was performed to study the influence of a full drop volume decrease/increase cycle on surface tension. In this experiment the drop volume was first decreasing and after the drop reached an almost spherical shape it started to increase.

As one can see from Figs. 5-7 only at comparatively small bubble volumes, i.e. when the bubble shape is close to spherical one, the experimental results show a large scattering. This is in accordance with the results of other authors [10]. All larger volumes are acceptable for surface tension measurements. For example, in the

experiment shown in Fig. 7 the range of volume changes corresponding to acceptable results is between 25mm^3 and 40mm^3 i.e. with $\pm 23\%$ of relative change in respect to average value of $32,5\text{mm}^3$.

In order to study the dependence of surface tension on drop volume for liquids with low surface tension we performed experiments similar to first one (see Fig. 5) but with a 2mmol/l solution of Triton-X100 which is a highly surface active surfactant with a critical micelle concentration of about $0,25\text{mmol/l}$ (see Fig. 8). As one can see for this liquid with low surface tension the type of dependence $\gamma(V_d)$ is almost the same as that of the first experiment.

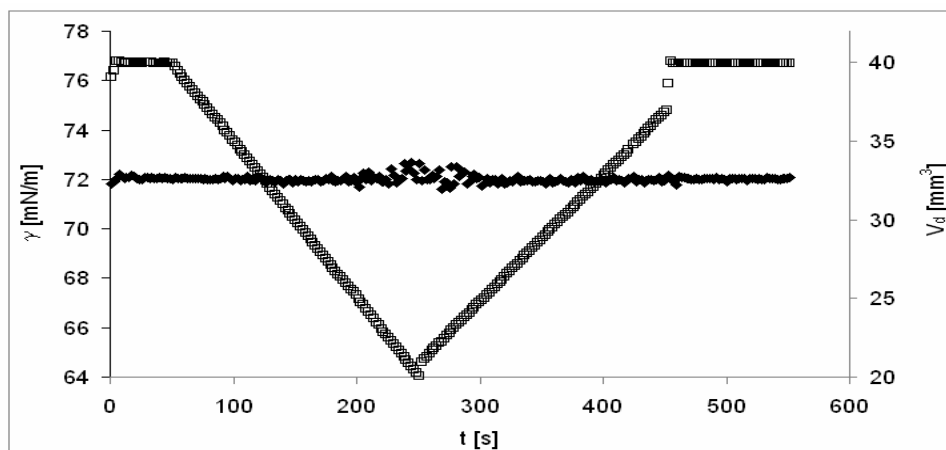


Figure 7 – Dependence of surface tension g and pendant drop volume V_d of pure water as a function of time t for decreasing/increasing volume; symbols are: (\circ) surface tension, (\square) drop volume

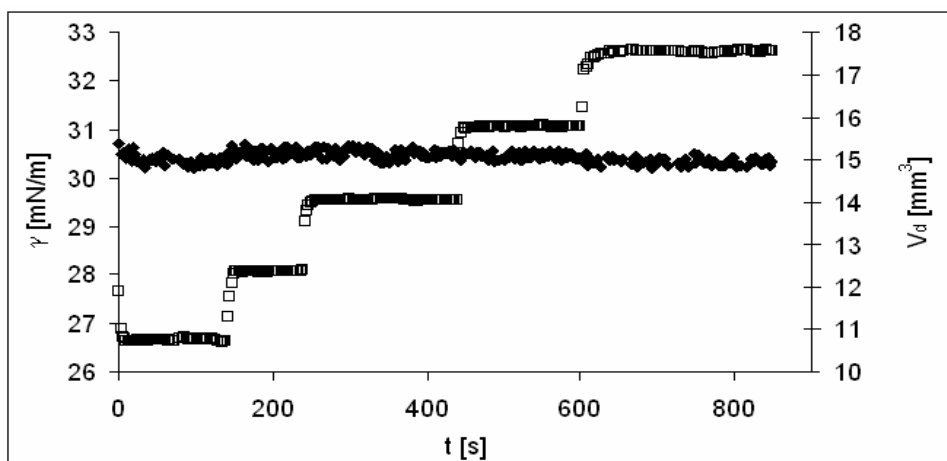


Figure 8 – Dependence of surface tension g and buoyant bubble volume V_d of a 2mmol/l solution of Triton-X100 as a function of time t for increasing volume; symbols are: (\circ) surface tension, (\square) bubble volume

All these results indicate that proposed method of surface tension measurement is well suitable for experiments with oscillations of drop/bubble area with a relative are change of about $\pm 7-10\%$.

It should be noted here that the analysis of axisymmetric profiles is more suitable for measuring surface tension by elongated drops/bubbles rather than flattened ones. This is because the elongated profiles have usually a larger deviation from a sphere and thus the sensitivity of

the shape to surface tension changes $\xi = \partial V / \partial \gamma$ (or partial derivative of another characteristic shape parameter) is considerably higher than that of flattened profile. Thus, both types of elongated shapes – pendant drop and buoyant or emerging bubble – should preferably be used for accurate surface tension measurements. Note, however, buoyant or emerging bubbles are more convenient, as compared to pendant drops, for

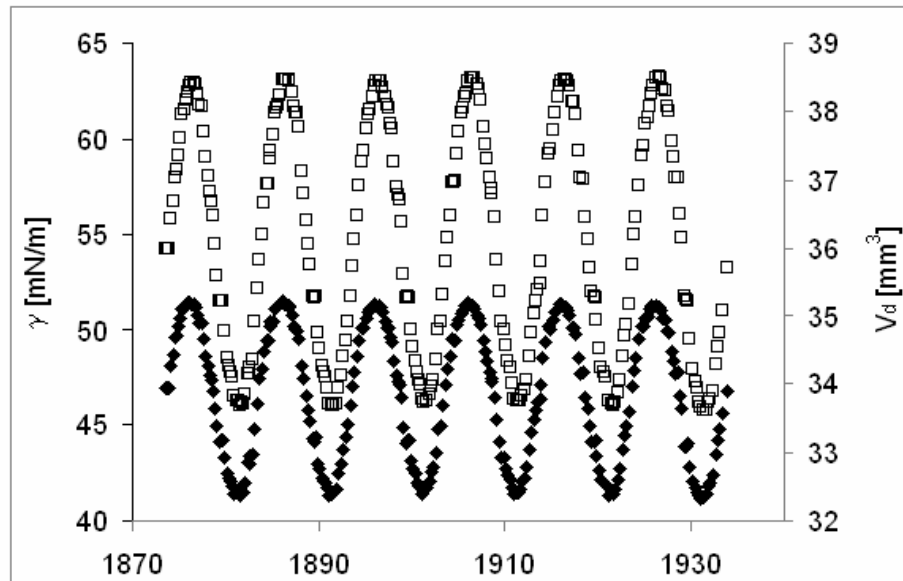


Figure 9 – Dependence of surface tension γ and pendant drop volume V_d of an oral fluid at an applied frequency pf 0,1 Hz; symbols are: (◊) surface tension, (◻) drop volume

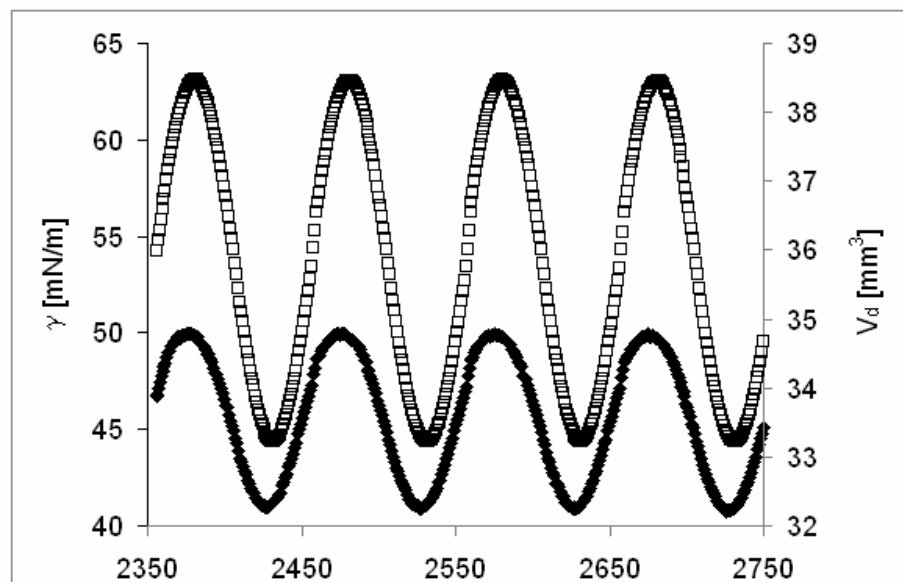


Figure 10 – Dependence of surface tension γ and pendant drop volume V_d of an oral fluid at an applied frequency of 0,01 Hz; symbols are: (◊) surface tension, (◻) drop volume

studies of highly surface active surfactants at low total bulk concentrations, because the depletion of the bulk surfactant concentration due to adsorption of surfactant molecules at the bubble surface is negligible. This depletion effect is considerable in pendant drop experiments and can be used for a direct estimation of the adsorbed amount of surfactants [13].

Harmonic oscillations of the drop/bubble area can be used to get parameters of the surface visco-elasticity of a studied liquid [12], which provides useful information about the mechanisms of possible interfacial relaxation processes. Such experiments with oscillations require that the error in surface tension measurement would be much less than the amplitude of surface tension oscillation. In order to check the validity of our algorithm in this situation an experiment with an oral fluid (saliva) of a female patient with an autoimmune thyroiditis was performed. Its result is shown in Figs. 9 and 10 for an applied frequency 0,1 Hz and 0,01 Hz, respectively. The dependence of $\gamma(V_d)$ for the oral fluid clearly shows that the proposed algorithm of surface tension measurement can be successfully used in experiments with oscillations as well. For instance, the parameters of surface visco-elasticity can be estimated from these results via the Eqs. (12)–(13) [12]

$$E = A_0 \frac{\Delta\gamma}{\Delta A}, \quad (12)$$

$$\varphi = \varphi_\gamma - \varphi_A, \quad (13)$$

where E is a visco-elasticity modulus, φ is a phase shift, A_0 is an average value of the surface area, ΔA and $\Delta\gamma$ are amplitudes of changes of surface area and surface tension, respectively, and φ_A and φ_γ are initial phases of each oscillation. Thus, for the frequency 0,1 Hz the results are $E=76,3$ mN/m, $\varphi=10,4^\circ$, and for the frequency 0,01 Hz we get $E=61,9$ mN/m, $\varphi=16,8^\circ$.

CONCLUSION

There are various possibilities to improve the standard technique for measuring surface or interfacial tension by drop and bubble profile analysis. One possibility to increase the accuracy is the fitting of experimental grey level gradients obtained from experimental drop or bubble images to normal distribution functions and locate the edge into the maximum of the distribution. During fitting of the Gauss-Laplace equation to an experimental profile many algorithms require interpolation between theoretical points to calculate the target function. The proposed algorithm of calculation of the distance between drop image edge coordinates and the theoretical profile considerably improves the convergence of the optimization procedure used in the main calculation algorithm. The stability of

measurement results allows using this technique in experiments with oscillations at small frequencies.

1. A.W. Adamson, *Physical Chemistry of Surfaces*, 5th ed., New York: John Wiley & Sons, 1990. 2. Bashforth F., Adams J.C., *An Attempt to Test the Theories of Capillary Action*, Cambridge: University Press, 1883, 140 p. 3. Rotenberg, Y., Boruvka, L. and Neumann, A.W. "Determination of Surface Tension and Contact Angle from the Shapes of Axisymmetric Fluid Interfaces", *J. Colloid Interface Sci.* 93, pp. 169-183, 1983. 4. Knuth D., *The Art of Computer Programming, Volume 3: Sorting and Searching*, 3rd ed., Addison-Wesley, 1997. 5. Zholob S.A., Makievski A.V., Miller R. and Fainerman V.B., *Advances in calculation methods for the determination of surface tensions in drop profile analysis tensiometry*, in "Bubble and Drop Interfaces", Vol. 2, *Progress in Colloid and Interface Science*, R. Miller and L. Liggieri (Eds.), Brill Publ., Leiden, 2011, 39-60. 6. Press W.H., Teukolsky S.A., Vetterling W.T., Flannery B.P. (2007), *Numerical Recipes: The Art of Scientific Computing*, 3rd ed., New York: Cambridge University Press, ISBN 978-0-521-88068-8. 7. Levenberg K., *A Method for the Solution of Certain Non-Linear Problems in Least Squares*, *The Quarterly of Applied Mathematics*, 2 (1944) 164. 8. Marquardt D., *An Algorithm for Least-Squares Estimation of Nonlinear Parameters*, *SIAM Journal on Applied Mathematics*, 11 (1963) 431. 9. S. Brandt, *Data Analysis*, 3rd ed., New York: Springer, 1999. 10. Sameh M.I.Saad, Polikova Z., Neumann A.W., *Colloids and Surface A, Physicochem. Eng. Aspects*, 384(2011)442-452. 11. R. Miller, C. Olak and A.V. Makievski, *SÖFW-Journal*, 130 (2004) 2. 12. Zholob S.A., Kovalchuk V.I., Makievski A.V., Krägel J., Fainerman V.B. and Miller R., *Determination of the dilational elasticity and viscosity from the surface tension response to harmonic area perturbations*, in "Interfacial Rheology", Vol. 1, *Progress in Colloid and Interface Science*, R. Miller and L. Liggieri (Eds.), Brill Publ., Leiden, 2009, p. 77-102. 13. V.B. Fainerman and R. Miller, *Direct determination of protein and surfactant adsorption by drop and bubble profile tensiometry*, in "Bubble and Drop Interfaces", Vol. 2, *Progress in Colloid and Interface Science*, R. Miller and L. Liggieri (Eds.), Brill Publ., Leiden, 2011, p. 179-193.

Поступила в редакцію 15.11.2012р.

Рекомендував до друку докт. техн. наук,
проф. Кісіль І. С.